

Article

Adsorption Characteristics of Carbon Monoxide on Ag- and Au-Doped HfS₂ Monolayers Based on Density Functional Theory[†]

Guochao Qian^{1,2}, Weiju Dai¹, Fangrong Zhou¹, Hongming Ma¹, Shan Wang¹, Jin Hu¹ and Qu Zhou^{3,*} 

¹ Electric Power Science Research Institute of Yunnan Power Grid Co., Ltd., Kunming 650217, China; zm18973102153@163.com (G.Q.); dwj0479@163.com (W.D.); zhfr0508@sina.com (F.Z.); 15912539853@126.com (H.M.); ws1smirage@sina.com (S.W.); i23456789jkl@163.com (J.H.)

² State Key Laboratory of Power Transmission Equipment and System Security and New Technology, College of Electrical Engineering, Chongqing University, Chongqing 400044, China

³ College of Engineering and Technology, Southwest University, Chongqing 400715, China

* Correspondence: zhouqu@swu.edu.cn

[†] This paper is an extended version of our paper published in the 16th Annual Conference of China Electrotechnical Society (ACCES 2021), Beijing 10000, China, September 2021.

Abstract: A large amount of power equipment works in closed or semi-closed environments for a long time. Carbon monoxide (CO) is the most prevalent discharge gas following a fault in the components. Based on the density functional theory of first principles, the adsorption behavior of CO gas molecules on intrinsic, Ag-doped and Au-doped hafnium disulfide (HfS₂) monolayers was systematically studied at the atomic scale. Firstly, the intrinsic HfS₂ monolayer, Ag-doped HfS₂ (Ag-HfS₂) monolayer and Au-doped HfS₂ (Au-HfS₂) monolayer, with different doping sites, were created. The structural stability, dopant charge transfer, substrate conductivity and energy band structure of different doping sites of the Ag-HfS₂ and Au-HfS₂ monolayer structures were calculated. The most stable doping structure was selected with which to obtain the best performance on the subsequent gas adsorption test. Then, the CO adsorption models of intrinsic HfS₂, Ag-HfS₂ and Au-HfS₂ were constructed and geometrically optimized. The results show that the adsorption energy of the Ag-HfS₂ monolayer for CO gas is −0.815 eV, which has good detection sensitivity and adsorption performance. The adsorption energy of CO on the Au-HfS₂ monolayer is 2.142 eV, the adsorption cannot react spontaneously, and the detection sensitivity is low. The research content of this paper provides a theoretical basis for the design and research of gas sensing materials based on HfS₂, promoting the development and application of HfS₂ in gas sensing and other fields.

Keywords: density functional theory; HfS₂; doping; CO; gas sensing



Citation: Qian, G.; Dai, W.; Zhou, F.; Ma, H.; Wang, S.; Hu, J.; Zhou, Q. Adsorption Characteristics of Carbon Monoxide on Ag- and Au-Doped HfS₂ Monolayers Based on Density Functional Theory. *Chemosensors* **2022**, *10*, 82. <https://doi.org/10.3390/chemosensors10020082>

Academic Editor: Andrea Ponzoni

Received: 4 January 2022

Accepted: 1 February 2022

Published: 15 February 2022

Publisher's Note: MDPI stays neutral with regard to jurisdictional claims in published maps and institutional affiliations.



Copyright: © 2022 by the authors. Licensee MDPI, Basel, Switzerland. This article is an open access article distributed under the terms and conditions of the Creative Commons Attribution (CC BY) license (<https://creativecommons.org/licenses/by/4.0/>).

1. Introduction

In recent years, as people pay more attention to air pollution and public health, the requirements for high sensitivity and online detection in the field of gas sensor research have become more and more demanding [1,2]. A large amount of electrical equipment works in closed or semi-closed environments for a long time. Liu et al. designed three different defect models to simulate the common discharge fault types of power equipment [1]. Experiments show that CO is the gas component with the highest concentration in the discharged gas under various conditions. It is flammable and highly toxic, endangering human life and health.

After the successful preparation of graphene through micromechanical exfoliation, two-dimensional materials have shown great potential in various applications due to their excellent properties, especially in the field of sensing materials, which has attracted the attention of many researchers [3–6]. Transition metal dihalides (TMDs) are a new type

of layered compound. TMDs have an ABA-type atomic stacking sequence, in which one metal plane atom is contained in two chalcogen atom planes [7–9]. When TMDs are confined to a single nanosheet, their electronic behavior will change significantly, appearing as direct band gap semiconductors, which greatly expands their application range in nanoelectronics [10–13]. At present, many studies in the field of TMDs gas sensors have proposed some sensing materials based on MoX_2 ($X = \text{S}, \text{Se}$ and Te) monolayers [14–18]. In the choice of transition metals (TM), such as Si or Ge, compared with traditional semiconductors, the carrier mobility is lower, and the uneven surface film hinders their sensing applications to a certain extent [19,20]. On the contrary, HfX_2 ($X = \text{S}, \text{Se}, \text{Te}$) compounds are considered to be small band gap semiconductors with large work function values, high electron affinity and reasonable carrier mobility, which makes them useful in many fields, such as nanoelectronics and optoelectronics [21,22]. The metal doping on TMDs has been recognized as an effective method to adjust their electronic properties, so as to further study their adsorption of gas molecules and the optimization of their sensing performance [23–26]. Yuwen et al. have completed the doping of Ag and Au on MoS_2 monolayers to optimize its gas sensing performance [27]. Michael Schmidt et al. found that HfS_2 and HfSe_2 have stronger gas sensitivity than MoS_2 , MoSe_2 and MoTe_2 when interacting with oxygen molecules and water molecules, and are more suitable for use as gas-sensitive materials in the surrounding environment [28]. Chen et al. studied the adsorption performance of intrinsic HfS_2 for SO_2 , HF, SO_2F_2 and H_2S gases under certain conditions [29]. However, there is no research on the sensitivity characteristics of CO gas, and there are few studies on metal-doped HfS_2 .

In this paper, first-principles density functional theory is used to study the most stable configuration of intrinsic HfS_2 , Ag- HfS_2 and Au- HfS_2 single-layered structures. We analyze their adsorption results and adsorption performance for harmful CO gas, comprehensively consider the adsorption parameters, adsorption energy change, density of state (DOS) and atomic charge density distribution (ELF), and explore the possibility of HfS_2 functioning as a new nano-sensing material. The research content of this paper provides theoretical guidance for further discussion on the application of Ag- HfS_2 and Au- HfS_2 monolayers in the field of gas sensing.

2. Materials and Methods

All calculations in this paper use the Dmol³ module of Materials Studio software, version 8.0. The first principles mainly include two branches: density functional theory and molecular dynamics. The Dmol³ module is based on density functional theory. It is a self-consistent calculation process that can comprehensively analyze the adsorption behavior of gas–solid surfaces [30]. Considering the calculation speed, a periodic supercell model was established to replace the infinite number of plane atoms in the two-dimensional material. The supercell model is divided into a vacuum layer and a crystal layer [31,32]. In order to avoid the influence of the interaction between adjacent layers, the thickness of the vacuum layer is set to 20 Å. Perdew–Burke–Ernzerhof (PBE) is selected as the generalized gradient approximation (GGA) of the exchange correlation potential energy, and the bi-numerical orbital basis set +p orbital polarization function (DNP) is used to calculate the electronic pseudopotential [33]. DNP also is set as the basis function of linear combination of atomic orbitals (LCAO). In all calculations, the electron spin is not restricted [34].

Taking into account the influence of van der Waals forces between molecules, the DFT-D2 method is used to analyze all models. The energy convergence accuracy, the stress convergence standard and the maximum allowable displacement are set to 10^{-5} Ha, 2×10^{-3} Ha/Å and 5×10^{-3} Å, respectively. In addition, the cut-off radius of all models is set to 5 Å, and the widening is set to 0.005 Ha. When calculating the geometric structure and electronic properties of the system, the k value of Monkhorst–Pack is set to $7 \times 7 \times 1$, so that the physical and chemical parameters of the adsorption system (geometric structure and electronic properties) can be accurately obtained. Layout refers to the distribution of

electrons on each atomic orbit. Analyzing the layout can help us to understand the bonding of atoms in the molecule. This article uses the Mulliken charge analysis method.

We calculate the adsorption capacity of HfS₂ material for gas, expressed as the adsorption energy (E_{ad}) as follows:

$$E_{ad} = E_{X-HfS_2/gas} - E_{X-HfS_2} - E_{gas} \quad (1)$$

Among them, $E_{X-HfS_2/gas}$ and E_{X-HfS_2} are the total energy of the system before and after the gas is adsorbed, and X represents metal doping. There is no X when calculating the undoped HfS₂ monolayer. E_{gas} is the energy of the adsorbed gas molecules.

In order to analyze whether gas molecules donate or provide electrons in the adsorption reaction, the charge transfer amount Q_t is:

$$Q_t = Q_{adsorbed(gas)} - Q_{isolated(gas)} \quad (2)$$

$Q_{adsorbed(gas)}$ and $Q_{isolated(gas)}$ are the amount of charge after the gas is adsorbed and before it is adsorbed, respectively. If Q_t is positive, it means that gas molecules are charge acceptors; otherwise, gas molecules are charge donors.

In this paper, E_{ad} , adsorption distance, band structure, total density of states (TDOS), partial density of states (PDOS) and transfer charge are studied to judge the strength of adsorption, in order to analyze the sensitivity and selectivity of the substrate material to gas and the feasible methods to enhance the adsorption.

The energy band structure is one of the most commonly used pieces of information calculated by the first-principles method, and it can be divided into three parts: the valence band, band gap and conduction band. For semiconductors, in the ground state, electrons start to fill up from the lowest energy level, and just fill up to a certain energy band. The one with the highest energy in the full band is called the valence band. After that, the empty band part is the band gap, and the band gap width (energy) of the semiconductor is relatively small. Therefore, the electrons in the valence band may transition to the next energy band after being injected with a photoelectric stimulus or after being thermally excited. The electrical properties are prone to major changes. As shown in Figure 1, we use a semiconductor HfS₂ monolayer structure with a band gap of 1.198 eV, which is consistent with previous studies.

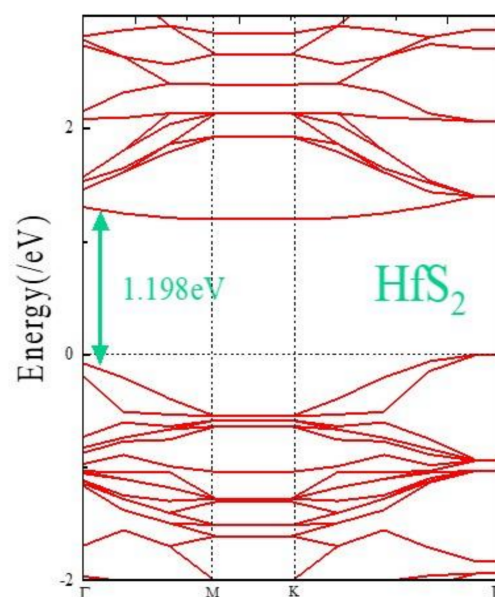


Figure 1. Band structure of intrinsic HfS₂ monolayer.

The calculation result of DOS is related to the calculation accuracy. The principle of Dmol³ calculation integration is a simplified linear interpolation method, which gives the DOS graph a slight tailing part. When selecting a smaller smearing width (smearing value), more accurate results will be obtained, but dense spikes will be produced, which will affect the analysis of the results. When a larger smearing value is selected, the image will be too smooth, and many details will be lost. Therefore, the smearing value set in this paper is 0.1 eV, which has a certain error from the theoretical value, but it is also within a reasonable range.

3. Results and Discussion

3.1. Metal Doping Method Selection

First, a geometric optimization model of the single-layer HfS₂ structure was established. The doping behavior of Ag on the single-layer film was studied. Two doping methods are considered to replace Hf atoms or S atoms with doped metal atoms. The optimized structure of the intrinsic HfS₂ monolayer is shown in Figure 2(a1,a2), where (a1) is the top view, and (a2) is the side view. The intrinsic HfS₂ monolayer is an ABA-type structure similar to MoS₂. With a layer of hafnium atoms sandwiched between two sulfur layers, the S-Hf bond length is 2.556 Å. Figure 2(a3) is the ELF of HfS₂. The blue indicates the depletion of electrons, and the red indicates the accumulation of electrons. It can be seen that in the HfS₂ monolayer structure, Hf atoms are electron donors, and S atoms are electron acceptors.

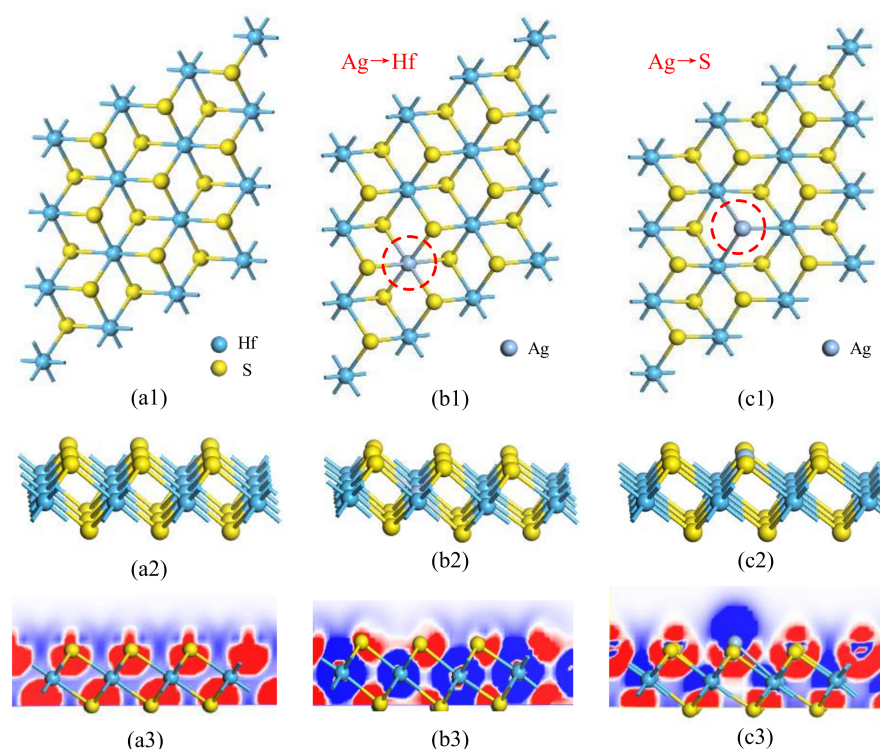


Figure 2. Geometric structures and ELF of intrinsic and Ag-HfS₂ monolayer. (a) HfS₂; (b) Ag-HfS₂(Ag-Hf); (c) Ag-HfS₂(Ag-S).

For the Ag-HfS₂ monolayer, Figure 2b shows the replacement of Hf atoms with Ag atoms (Ag-Hf) to complete the doping, and Figure 2c shows the replacement of S atoms with Ag atoms (Ag-S) for doping. The S-Hf bond length before doping is 2.560 Å, which is consistent with previous findings [29]. The bond lengths of Ag-S and Ag-Hf after doping are 2.511 Å and 2.949 Å, respectively, which are not much different from the bond lengths of S-Hf. It proves that Ag atoms can be doped to form chemical bonds on the surface of HfS₂, as shown in Figure 2b, meaning that the Ag-Hf method is more stable. From Figure 2(b3),

it can be seen that the dopant Ag atom is slightly smaller than the electron depletion layer around the Hf atom, indicating that it is also an electron donor and provides slightly fewer electrons than the Hf atom. In Figure 2(c3), the Ag atom is also surrounded by dense positive charges, which shows that its behavior as an electron donor has nothing to do with the doping mode.

Figure 3 is a comparison diagram of the geometric structure and charge density distribution of intrinsic and Au-HfS₂ monolayers. In order to compare the adsorption performance of the same gas without the doping atoms under the same conditions, the same doping method as Ag atoms is adopted. Figure 3a shows the intrinsic HfS₂ monolayer structure, and Figure 3b shows the Au-HfS₂ monolayer after the replacement of the Au and Hf atoms (Au-Hf). The doped Au-S bond length is 2.481 Å. Figure 3c shows the Au-HfS₂ monolayer after the replacement of Au atoms with S atoms (Au-S), and the Au-Hf bond length is 2.863 Å. As shown in the side view, it can be seen that the Au atoms are slightly higher than the S atomic layer. The comparison proves that the Au-Hf bond length in Figure 3b is closer to the S-Hf bond length, and the difference is slightly larger than the difference between the Ag-Hf bond and the S-Hf bond. Therefore, for Au dopants, the Au-Hf method has a more stable geometric structure, and Au atoms can form chemical bonds in HfS₂. In Figure 3(b3,c3), the Au atoms in both doping modes are surrounded by dense positive charges, acting as electron donors in the substrate.

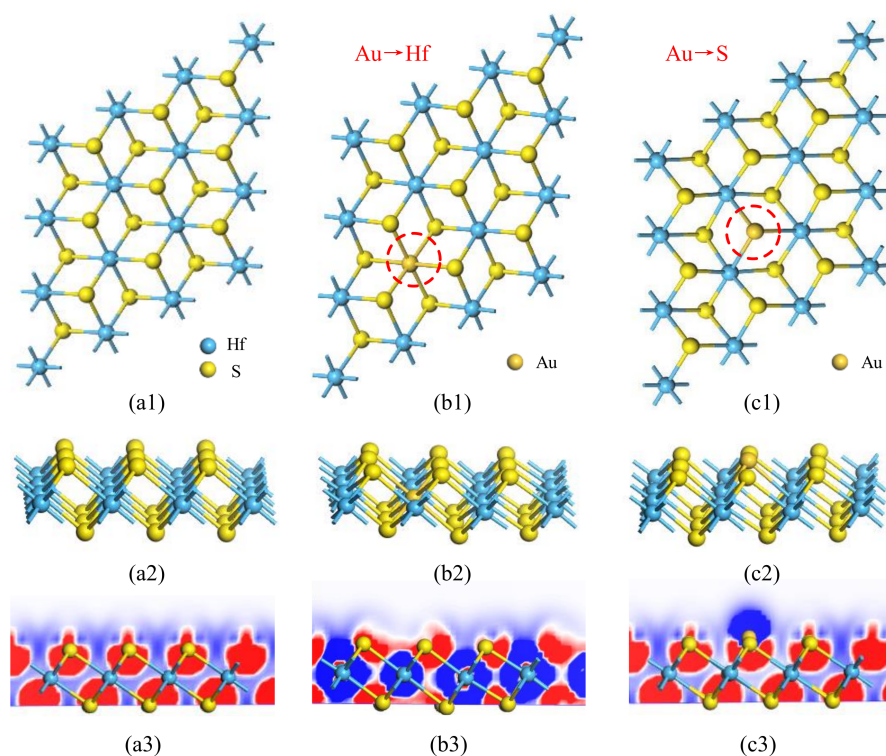


Figure 3. Geometric structures and ELF of intrinsic and Au-doped HfS₂ monolayer. (a) HfS₂; (b) Au-HfS₂(Au-Hf); (c) Au-HfS₂(Au-S).

Figure 4 compares the DOS diagram for the HfS₂ monolayer doped with Ag atoms. The dotted line is the zero value of the DOS, which represents the Fermi level. The Fermi level is the highest energy level that is filled with electrons when the energy band is at absolute zero. In Figure 4(a1), compared with the intrinsic HfS₂ represented by the black line, the TDOS curve of Ag-HfS₂ has undergone a significant deformation. An obvious peak appears near the Fermi level, indicating that the doping of Ag atoms will reduce the band gap of the HfS₂ monolayer, and the electrons will be easier to transfer between the valence band and the conduction band. Combined with the analysis of its geometric structure

parameters, the Ag-Hf replacement structure is selected for subsequent calculation and analysis. Figure 4(a2) shows the PDOS diagrams of the Hf-5d, S-3p and Ag-4d orbitals. It can be observed that Ag doping has a greater influence on the states below the Fermi level, which appear as occupied states. The spin-up and spin-down symmetry of each system indicates that both intrinsic HfS₂ and Ag-HfS₂ are non-magnetic systems. There is a slight hybridization between the Ag-4d and Hf-5d orbitals between -7.5 eV and -2.5 eV, indicating that there is a small charge transfer between Ag doped atoms and HfS₂.

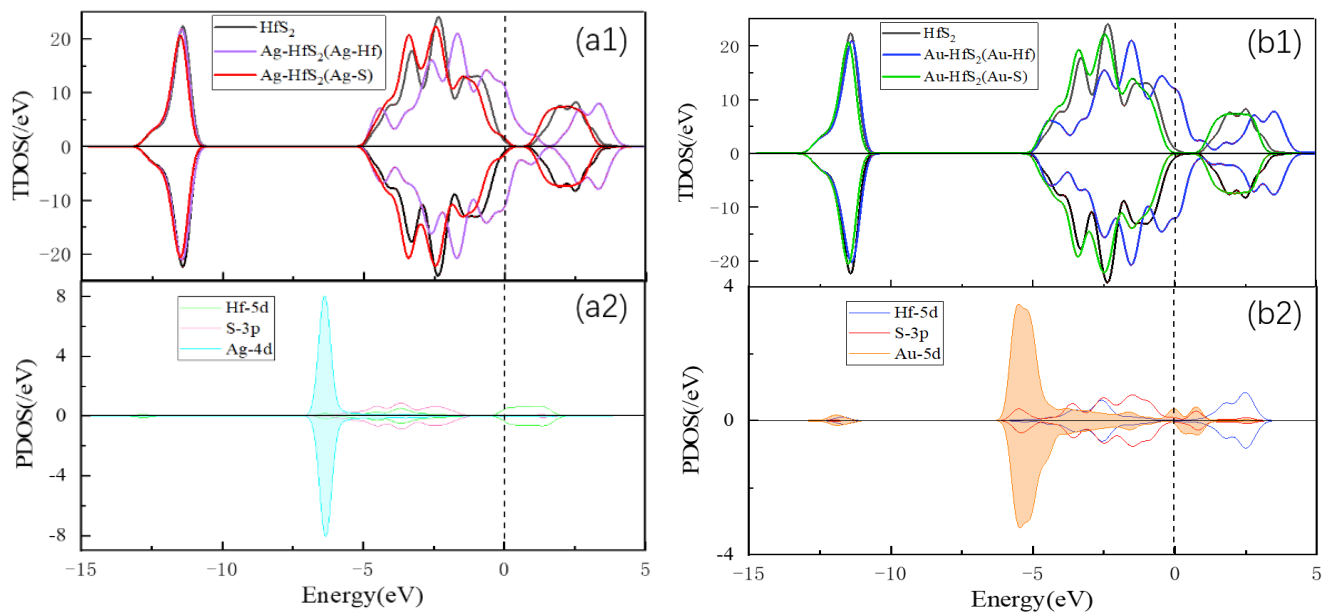


Figure 4. DOS of intrinsic and Ag/Au-doped HfS₂ monolayer. (a) Ag-HfS₂ system, (b) Au-HfS₂ system.

In Figure 4b, Au-HfS₂ is compared with intrinsic HfS₂. It can also be seen that with the Au-Hf method, the TDOS curve is more deformed, and the peak value at the Fermi level increases significantly. In summary, the Au-HfS₂ structure in Figure 3b is selected for subsequent calculations and analysis. The TDOS diagrams of the two doping atoms are very similar, indicating that the same group of elements, as doping atoms, have roughly the same effect on the system density of states of the base material, which is consistent with the results of the previous literature [35,36]. In Figure 4(b2), it can be observed that Au-5d and S-3p orbitals exhibit obvious hybridization behaviors near -5.5 eV, -1.8 eV and 1.1 eV. It shows that Au and S atoms form a stable doped structure, and the interaction with the HfS₂ monolayer is very strong.

The symmetry of DOS in Figure 4 shows that each system is a non-magnetic system. Figure 5 only plots the energy band structure of Ag-HfS₂ and the Au-HfS₂ single-layer spin-up. Both the bottom of the conduction band and the top of the valence band of the two systems are located at the Γ point, and the band gap is not 0, indicating that the doping of Ag and Au will not change the semiconductor properties of HfS₂. The band gaps of Ag-HfS₂ and Au-HfS₂ are 0.047 eV and 0.25 eV, respectively, which are much smaller than the 1.198 eV band gap of intrinsic HfS₂. After doping, the conductivity of the substrate is improved, and the Ag dopant has a greater influence on the conductivity.

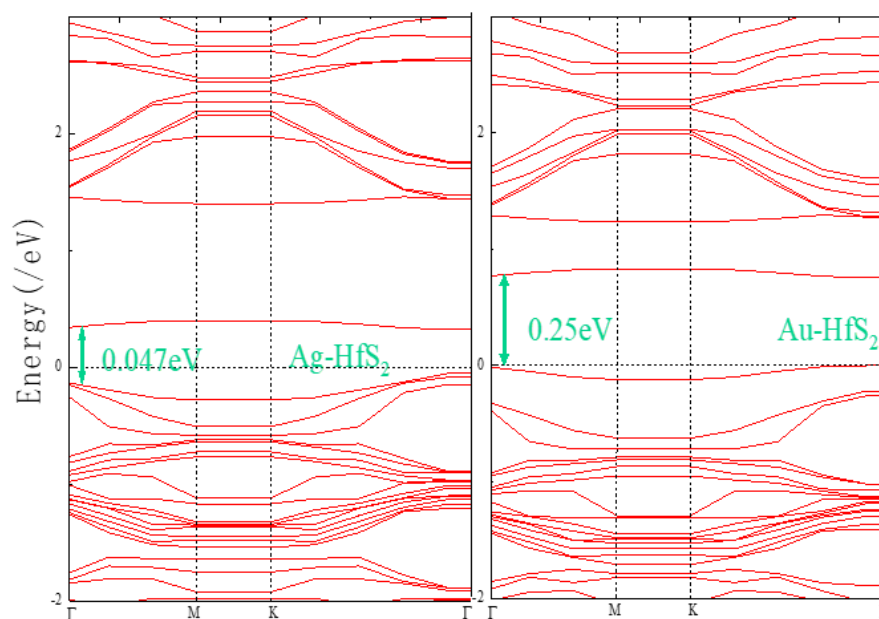


Figure 5. Band structures of Ag-HfS₂ and Au-HfS₂.

3.2. Adsorption Performance Analysis

A CO adsorption model was established with the intrinsic HfS₂ monolayer and the doped structure, and its adsorption performance was calculated. The calculation results of E_{ad} , adsorption distance (d) and Q_t are listed in Table 1. It can be seen that the energy transfer of the intrinsic HfS₂ adsorption of CO is very weak. The E_{ad} of Ag-HfS₂/CO is greater than 0.6, which reflects chemical adsorption, which is much stronger than the adsorption capacity of the intrinsic materials. The adsorption distances (D) listed in Table 1 are all the direct distances between the C atoms in CO and the nearest S atoms. It can be seen that the doped system effectively shortens the distance between the gas molecules and the substrate material. The transfer charges of HfS₂/CO and Ag-HfS₂/CO are both positive, indicating that gas molecules lose electrons, and a reduction reaction occurs. The greater the charge transfer, the stronger the atomic hybridization. It can be inferred that Ag doping effectively enhances the charge transfer between the CO molecules and the HfS₂ surface. The Q_t of the Au-HfS₂/CO system is negative, and electrons are transferred from the base material to the gas molecule.

Table 1. Adsorption parameters of each adsorption structure.

The Adsorption Configuration	D(Å)	E_{ad} (eV)	Q_t €
HfS ₂ /CO	C-S 3.568	−0.180	0.012
Ag-HfS ₂ /CO	C-S 1.589	−0.815	0.283
Au-HfS ₂ /CO	C-S 1.717	2.142	−0.336

Figure 6(a1) is a side view of the intrinsic HfS₂ adsorbing CO, showing that the adsorption distance is relatively far. According to the calculations, the C atoms in the C and O atoms are closer to the substrate material, so the C atoms are used as the adsorption sites when establishing the adsorption model of the doped structure. Figure 6(a2) shows the charge density distribution of intrinsic HfS₂ adsorbing CO. Blue represents positive charge and red represents negative charge. The charge transfer between the gas and substrate is very weak. Figure 6b is a diagram of the energy band structure of the HfS₂/CO system, with a band gap of 1.263 eV. It shows that the conductivity of the base material is improved to a certain extent after the gas is adsorbed, but the semiconductor properties are still maintained. Figure 6(c1) shows the DOS comparison of the entire system before and after

HfS₂ adsorbs CO. The two curves basically coincide. Figure 6(c2) is the DOS comparison before and after the CO gas molecule is adsorbed. After being adsorbed, the density of state curve shifts to the left, indicating that its electronic active state is reduced.

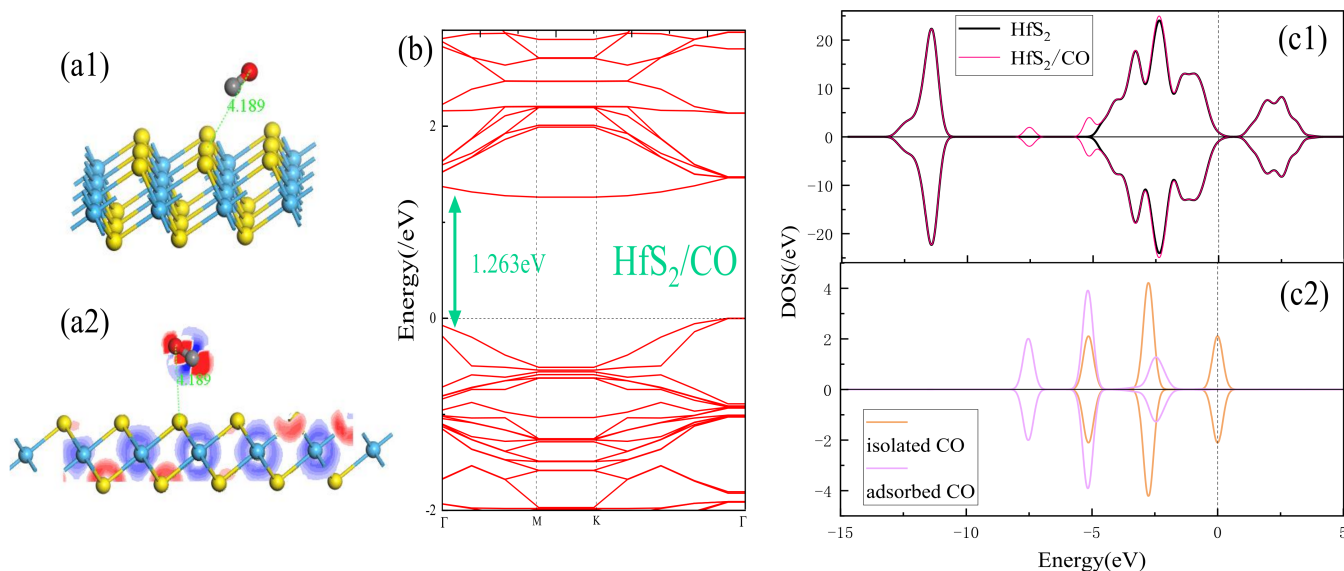


Figure 6. (a) Geometric structures and ELF; (b) B and structure; (c) DOS of CO adsorption on HfS₂ monolayer.

The structure, ELF, band structure and DOS curve of the Ag-HfS₂/CO adsorption system are shown in Figure 7. Figure 7(a1) shows that the S-Hf bond closest to the gas molecule has undergone a large deformation, and the bond length has changed from 1.142 Å to 3.598 Å, which verifies the obvious enhancement of E_{ad} in this system. The electron transfer from gas to Ag-HfS₂ is observed from the charge density between the C and S atoms, as shown in Figure 7(a2). The accumulation and depletion of electrons can be observed on the C-S bond, which means that a new chemical bond is formed between the carbon and sulfur atoms. From the energy band structure in Figure 7b, it can be observed that the band gap of the system is 0.265 eV, and there is no energy level that crosses the Fermi level. The adsorption of CO molecules did not change the semiconductor properties of the Ag-HfS₂ monolayer. According to the DOS of the CO molecule in Figure 7c, it can be inferred that the changes near the Fermi level are mainly due to the influence of the CO molecule. The adsorbed CO molecules move to the left of the energy, releasing the occupied state at the Fermi level. The electrical conductivity of the single layer material changes greatly. In other words, the Ag-HfS₂ monolayer film has good CO detection sensitivity.

The structure, charge density distribution, energy band structure and DOS curve of the Au-HfS₂/CO adsorption system are shown in Figure 8. Figure 8(a1) shows that the C-O bond has undergone a large deformation after the gas is adsorbed, and the bond length has changed from 2.556 Å to 2.465 Å. Figure 8b shows the energy band structure of the Au-HfS₂/CO system. The band gap is very small at 0.041 eV. Electrons can easily transition from the valence band to the conduction band, and the semi-conductivity of the substrate material cannot be determined. As shown in Figure 8c, the density of states of the adsorbed CO molecules is basically active on the left side of the Fermi level. In addition, the Au-5d orbital and the C-2p orbital have a certain hybridization, which means the stability of the chemical bond of Au-C. In summary, after the CO gas is adsorbed by the doped base material, the electron DOS has a large change, and all the atoms move to the side with lower energy.

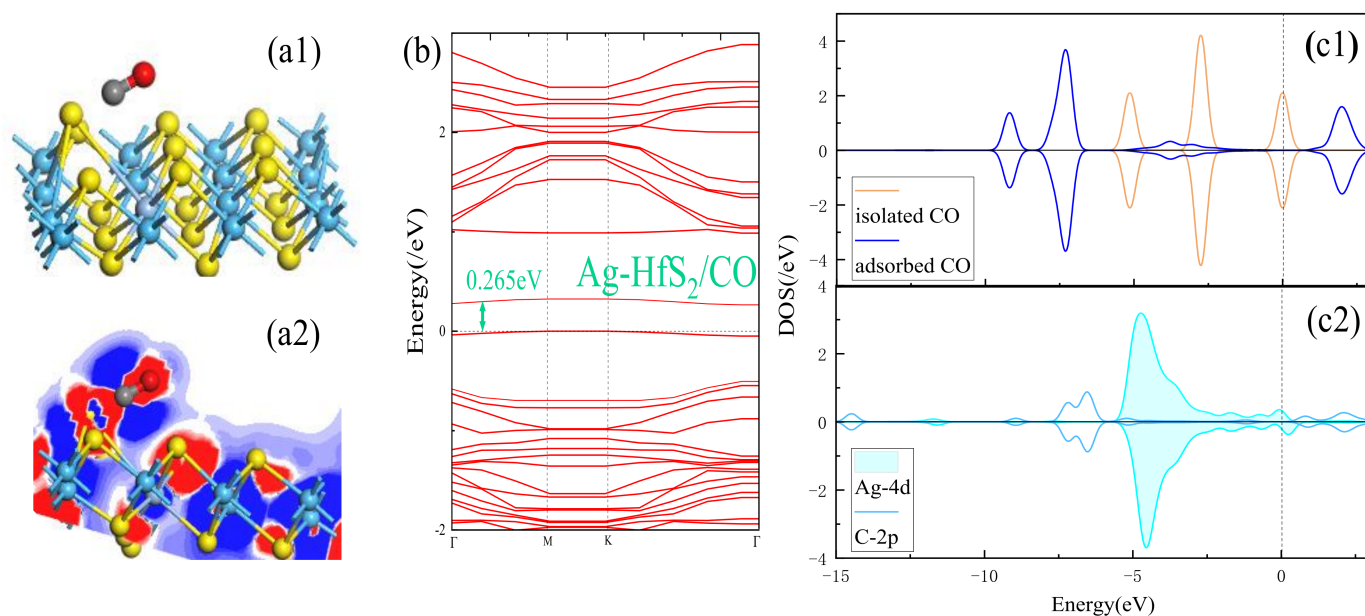


Figure 7. (a) Geometric structures, and ELF; (b) Band structure; (c) DOS of CO adsorption on Ag-HfS₂ monolayer.

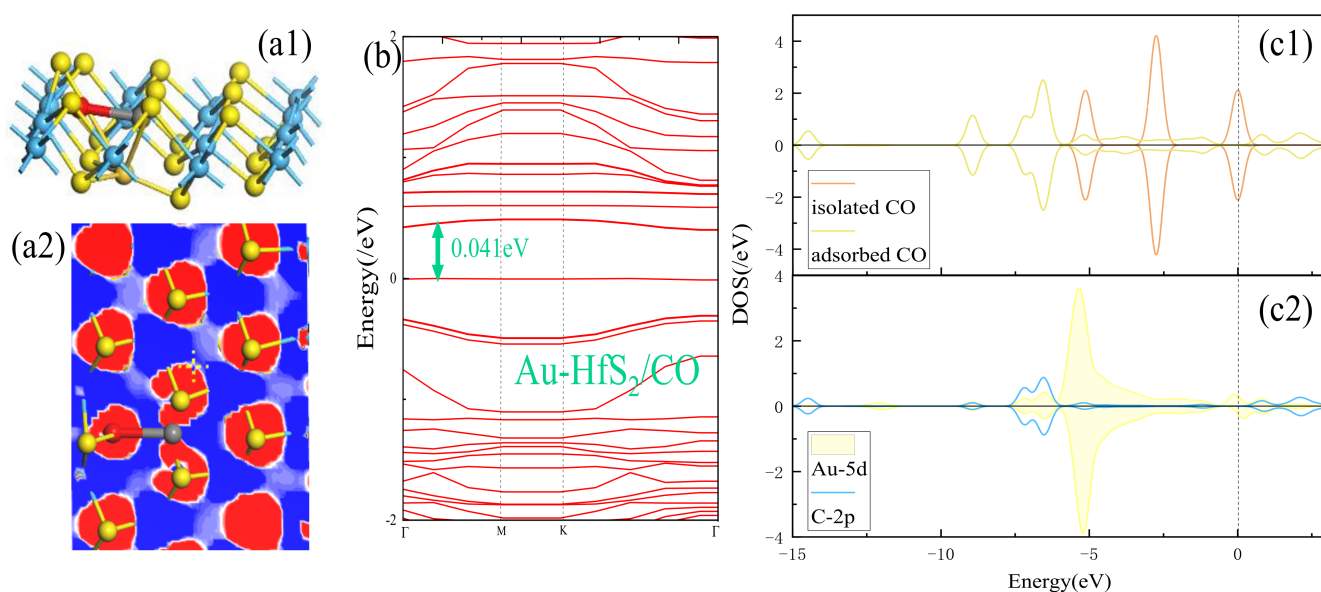


Figure 8. (a) Geometric structures and ELF; (b) Band structure; (c) DOS of CO adsorption on Au-HfS₂ monolayer.

4. Conclusions

Based on the first principles, this article discusses the regulation of the HfS₂ monolayer's adsorption characteristics for CO gas. The optimized structure of two doping methods of metal atoms is studied. The stability of Ag-HfS₂ after doping modification is discussed, and it is concluded that Ag-Hf is the most stable doping site. Subsequently, the adsorption optimization model of each substrate material was constructed, and the changes to the distance, energy, charge, DOS and energy band structure before and after adsorption were analyzed. The results show that the intrinsic HfS₂ structure has a longer adsorption distance for CO gas. The adsorption energy and charge transfer, at -0.180 eV and 0.012 eV, respectively, are weak. The DOS and band structure changes before and after adsorption are small. It is inferred that the interaction between the CO gas molecules and intrinsic

HfS₂ belongs to weak physical adsorption. The adsorption performance of the doped Ag atoms on HfS₂ is significantly improved. The adsorption energy and transfer charge of CO increase significantly. The DOS before and after adsorption changes obviously, and the fractional density map has more orbital hybridization. Among them, the adsorption energy of Ag-HfS₂/CO is -0.815 eV, which demonstrates stable chemical adsorption. The above research results indicate that the new Ag-HfS₂, as a two-dimensional material, has high sensitivity and adsorption to CO gas, and is suitable as a gas-sensitive material for CO gas detection.

Author Contributions: Conceptualization, G.Q. and W.D.; methodology, F.Z.; software, G.Q. and H.M.; data curation, G.Q., W.D. and S.W.; writing—original draft preparation, G.Q.; writing—review and editing, G.Q. and Q.Z.; supervision, J.H. and Q.Z.; project administration, Q.Z. All authors have read and agreed to the published version of the manuscript.

Funding: This research was funded by the National Natural Science Foundation of China, grant number 52077177 and The Fundamental Research Funds for the Central Universities, grant number XDJK2019B021.

Institutional Review Board Statement: Not applicable.

Informed Consent Statement: Not applicable.

Conflicts of Interest: We confirm that our work has no known competing financial interests or personal relationships that could have appeared to influence the work reported in this paper.

References

1. Liu, B.S.; Wang, D.; Ma, A.J.; Gui, Y.; Zhang, Q.S.; Zhang, J.; Gong, L.; Tian, M.; Wang, X.P. Study on the components of air under partial discharge condition in closed space. *Power Syst. Prot. Control.* **2021**, *49*, 21–28. (In Chinese)
2. Tao, S.Y.; Feng, Y.; Zhang, T.C.; Cai, H.W. High voltage switch cabinet partial discharge on-line monitoring device based on pulse current method. *Power Syst. Prot. Control.* **2019**, *47*, 145–149. (In Chinese) [[CrossRef](#)]
3. Sun, Y.F.; Liu, S.B.; Meng, F.L.; Liu, J.Y.; Jin, Z.; Kong, L.T.; Liu, J.H. Metal oxide nanostructures and their gas sensing properties: A review. *Sensors* **2012**, *12*, 2610–2631. [[CrossRef](#)] [[PubMed](#)]
4. Novoselov, K.S.; Geim, A.K.; Morozov, S.V.; Jiang, D.; Zhang, Y.; Dubonos, S.V.; Grigorieva, I.V.; Firsov, A.A. Electric field effect in atomically thin carbon films. *Science* **2004**, *306*, 666–669. [[CrossRef](#)]
5. Zhang, Y.H.; Han, L.F.; Xiao, Y.H.; Jia, D.Z.; Guo, Z.H.; Li, F. Understanding dopant and defect effect on H₂S sensing performances of graphene: A first-principles study. *Comput. Mater. Sci.* **2013**, *69*, 222–228. [[CrossRef](#)]
6. Feng, Z.H.; Yuan, X.; Chen, J.C.; Yu, Y.Y.; Zheng, S.J.; Zhang, R.; Li, Q.N.; Chen, X.J.; Sun, C.L.; Zhang, H.; et al. Highly sensitive MoTe₂ chemical sensor with fast recovery rate through gate biasing. *2D Materials* **2017**, *4*, 025018. [[CrossRef](#)]
7. Zhang, D.Z.; Wu, J.F.; Li, P.; Cao, Y.H. Room-temperature SO₂ gas-sensing properties based on a metal-doped MoS₂ nanoflower: An experimental and density functional theory investigation. *J. Mater. Chem.* **2017**, *5*, 20666–20677. [[CrossRef](#)]
8. Baek, J.; Yin, D.M.; Liu, N.; Omkaram, I.; Jung, C.; Im, H.; Hong, S.; Kim, S.M.; Hong, Y.K.; Hur, J.; et al. A highly sensitive chemical gas detecting transistor based on highly crystalline CVD-grown MoSe₂ films. *Nano Res.* **2017**, *10*, 2904. [[CrossRef](#)]
9. Abbasi, A.; Sardroodi, J. Adsorption of O₃, SO₂ and SO₃ gas molecules on MoS₂ monolayers: A computational investigation. *Apply Surf. Sci.* **2019**, *469*, 781–791. [[CrossRef](#)]
10. Wang, J.X.; Zhou, Q.; Lu, Z.R.; Gui, Y.G.; Zeng, W. Adsorption of H₂O molecule on TM (Au, Ag) doped-MoS₂ monolayer: A first-principles study. *Phys. E Low-Dimens. Syst. Nanostruct.* **2019**, *113*, 72–78. [[CrossRef](#)]
11. Chen, D.C.; Tang, J.; Zhang, X.X.; Li, Y.; Liu, H.J. Detecting decompositions of sulfur hexafluoride using MoS₂ monolayer as gas sensor. *IEEE Sens. J.* **2019**, *19*, 9–46. [[CrossRef](#)]
12. Zhang, D.Z.; Jiang, C.X.; Wu, J.F. Layer-by-layer assembled In₂O₃ nanocubes/flower-like MoS₂ nanofilm for room temperature for maldehyde sensing. *Sens. Actuators B Chem.* **2018**, *273*, 176–184. [[CrossRef](#)]
13. Wang, J.X.; Zhou, Q.; Lu, Z.R.; Wei, Z.J.; Zeng, W. Gas sensing performances and mechanism at atomic level of Au-MoS₂ microspheres. *Apply Surf. Sci.* **2019**, *490*, 124–136. [[CrossRef](#)]
14. Zhang, W.X.; Huang, Z.S.; Zhang, W.L.; Li, Y.R. Two-dimensional semiconductors with possible high room temperature mobility. *Nano Res.* **2014**, *7*, 1731–1737. [[CrossRef](#)]
15. Aretouli, K.; Tsipas, P.; Tsoutsou, D.; Marquez-Velasco, J.; Xenogiannopoulou, E.; Giamini, S.A.; Vassalou, E.; Kelaidis, N.; Dimoulas, A. Two-dimensional semiconductor HfSe₂ and MoSe₂/HfSe₂ van der Waals heterostructures by molecular beam epitaxy. *Appl. Phys. Lett.* **2015**, *106*, 699. [[CrossRef](#)]
16. Cheng, G.; Zhang, H.J.; Wang, W.; Colombo, L.; Wallace, R.M.; Cho, K. Band alignment of two-dimensional transition metal dichalcogenides: Application in tunnel field effect transistors. *Appl. Phys. Lett.* **2013**, *103*, 329.

17. Wu, P.; Yin, N.Q.; Li, P.; Cheng, W.J.; Min, H. The adsorption and diffusion behavior of noble metal adatoms (Pd, Pt, Cu, Ag and Au) on a MoS₂ monolayer: A first-principles study. *Phys. Chem. Chem. Phys.* **2017**, *19*, 20713–20722. [[CrossRef](#)] [[PubMed](#)]
18. Delley, B. From molecules to solids with the DMol3 approach. *J. Chem. Phys.* **2000**, *113*, 7756–7764. [[CrossRef](#)]
19. Tkatchenko, A.; DiStasio, R.A., Jr.; Head-Gordon, M.; Scheffler, M. Dispersion-corrected Møller-Plesset second-order perturbation theory. *J. Mater. Phys.* **2009**, *131*, 171.
20. Fonseca, G.; Handgraaf, J.; Baerends, E.; Bickelhaupt, F.M. Voronoi deformation density (VDD) charges: Assessment of the Mulliken, Bader, Hirshfeld, Weinhold, and VDD methods for charge analysis. *J. Comput. Chem.* **2004**, *25*, 189–210. [[CrossRef](#)]
21. Lugo-Solis, A.; Vasiliev, I. Ab initio study of K adsorption on graphene and carbon nanotubes: Role of long-range ionic forces. *Phys. Rev. B* **2007**, *76*, 235431. [[CrossRef](#)]
22. Casida, M.; Jamorski, C.; Casida, K.C.; Salahub, D.R. Molecular excitation energies to high-lying bound states from time-dependent density-functional response theory: Characterization and correction of the time-dependent local density approximation ionization threshold. *J. Chem. Phys.* **1998**, *108*, 4439–4449. [[CrossRef](#)]
23. Perdew, J.; Burke, K.; Ernzerhof, M. Generalized gradient approximation made simple. *Phys. Rev. Lett.* **1996**, *77*, 3865. [[CrossRef](#)] [[PubMed](#)]
24. Diego, C.A.; Nery, V.E.; Daniela, E.O. Fe-doped graphene nanosheet as an adsorption platform of harmful gas molecules (CO, CO₂, SO₂ and H₂S), and the co-adsorption in O₂ environments. *Appl. Surf. Sci.* **2018**, *427*, 227–236.
25. Yao, W.; Zhou, S.; Wang, Z.; Lu, Z.; Hou, C. Antioxidant behaviors of graphene in marine environment: A first-principles simulation. *Appl. Surf. Sci.* **2020**, *499*, 143962. [[CrossRef](#)]
26. Sun, S.S.; Meng, F.C.; Wang, H.Y.; Wang, H. Novel two-dimensional semiconductor SnP₃: Highest ability, tunable bandgaps and high carrier mobility explored using first-principles calculations. *Mater. Chem.* **2018**, *6*, 11890. [[CrossRef](#)]
27. Yuwen, L.H.; Xu, F.; Xue, B.; Luo, Z.M.; Zhang, Q.; Bao, B.Q.; Su, S.; Weng, L.X.; Huang, W.; Wang, L.H. General synthesis of noble metal (Au, Ag, Pd, Pt) nanocrystal modified MoS₂ nanosheets and the enhanced catalytic activity of Pd-MoS₂ for methanol oxidation. *Nanoscale* **2014**, *6*, 5762–5769. [[CrossRef](#)] [[PubMed](#)]
28. Michael, S. Air sensitivity of MoS₂, MoSe₂, MoTe₂, HfS₂ and HfSe₂. *J. Appl. Phys.* **2016**, *120*, 125102.
29. Chen, D.C.; Zhang, X.X.; Tang, J.; Li, Y.; Cui, Z.L.; Zhou, Q. Using Single-Layer HfS₂ as Prospective Sensing Device Toward Typical Partial Discharge Gas in SF₆-Based Gas-Insulated Switchgear. *IEEE Trans. Electron Devices* **2019**, *66*, 1557–9646. [[CrossRef](#)]
30. Chen, D.C.; Zhang, X.X.; Xiong, H.; Tang, J.; Xiao, S.; Zhang, D.Z. A First-Principles Study of the SF₆ Decomposed Products Adsorbed Over Defective WS₂ Monolayer as Promising Gas Sensing Device. *IEEE Trans. Device Mater. Reliab.* **2019**, *19*, 473–483. [[CrossRef](#)]
31. Wang, J.X.; Zhou, Q.; Xu, L.N.; Gao, X.; Zeng, W. Gas sensing mechanism of transformer oil decomposed gases on Ag-MoS₂ monolayer: A DFT study. *Phys. E Low-Dimens. Syst. Nanostruct.* **2020**, *118*, 113947. [[CrossRef](#)]
32. Liu, Y.P.; Zhou, Q.; Hou, W.J.; Li, J.; Zeng, W. Adsorption properties of Cr modified GaN monolayer for H₂, CO, C₂H₂ and C₂H₄. *Chem. Phys.* **2021**, *550*, 111304. [[CrossRef](#)]
33. Zeng, F.P.; Li, H.T.; Cheng, H.T.; Tang, J.; Liu, Y.L. SF₆ Decomposition and Insulation Condition Monitoring of GIE: A Review. *High Volt.* **2021**, *6*, 955–966. [[CrossRef](#)]
34. Zeng, F.P.; Feng, X.X.; Chen, X.Y.; Yao, Q.; Miao, Y.L.; Dai, L.J.; Li, Y.; Tang, J. First-principles analysis of Ti₃C₂T_x MXene as a promising candidate for SF₆ decomposition characteristic components sensor. *Appl. Surf. Sci.* **2022**, *578*, 152020. [[CrossRef](#)]
35. Yuan, J.H.; Yu, N.N.; Wang, J.F.; Xue, K.H.; Miao, X.S. Design lateral heterostructure of monolayer ZrS₂ and HfS₂ from first principles calculations. *Appl. Surf. Sci.* **2018**, *436*, 919–926. [[CrossRef](#)]
36. Kanazawa, T.; Amemiya, T.; Ishikawa, A.; Upadhyaya, V.; Tsuruta, K.; Tanaka, T.; Miyamoto, Y. Few-layer HfS₂ transistors. *Sci. Rep.* **2016**, *6*, 22277. [[CrossRef](#)]